NAL TR-901T

ISSN 0389-4010
UDC 533.6.011.3:
518.61

TECHNICAL REPORT OF NATIONAL AEROSPACE LABORATORY

TR-901T

Transonic Airfoil Design Based on the Navier-Stokes Equations to Attain Arbitrarily Specified Pressure Distribution —An Iterative Procedure——

Naoki HIROSE, Susumu TAKANASHI and Nobuhiro KAWAI

March, 1986

NATIONAL AEROSPACE LABORATORY

CHŌFU, TOKYO, JAPAN

Transonic Airfoil Design Based on the Navier-Stokes Equations to Attain Arbitrarily Specified Pressure Distribution*
——An Iterative Procedure——

Naoki HIROSE**, Susumu TAKANASHI** and Nobuhiro KAWAI**

ABSTRACT

An iterative procedure for transonic airfoil design based on the Navier-Stokes equations to attain arbitrarily specified pressure distributions is proposed in this paper. A transonic integral equation for the inverse problem for the correction term between the basic pressure distribution and the specified pressure distribution is formulated and is combined with a time-averaged Navier-Stokes airfoil analysis code. Shock wave and viscous effects including weak separation are properly evaluated in the analysis mode and therefore are effectively incorporated in the design procedure. Numerical results for a shockless pressure distribution and a supercritical pressure distribution are presented. A small number of iterative steps yield almost satisfactory airfoil geometry in practical point of view. The method is also applied to low speed airfoil designs and the results are shown.

概　　要

任意に指定した圧力分布を実現する，ナビエ・ストークス方程式に基づく遷音速翼型設計の反復的手順を提案する。本手順は，基本圧力分布と指定圧力分布との間の差に対する翼型形状修正項に関する逆問題の遷音速積分方程式による設計法と，翼型に対する高レイノルズ数遷音速流の時間平均ナビエ・ストークス解析コード，NSFOIL,との結合によって組立てられる。NSFOILはBeam-Warming-Stegerの陰的近似因子化（IAF）法に，陰的な翼，伴流境界条件化等の改良を加えた差分法を用いた解析法である。解析法は，衝撃波や弱い剥離を含む粘性効果を適切に評価することが可能であり，従って，設計手順に，これらの効果を正しく評価評価することができる。衝撃波無し圧力分布と超臨界圧力分布に対する数値解析例を示す。数回の反復によって，実用的に満足な翼型形状を得ることができた。本手順は低速翼型設計にも，より容易に適用することが出来る。その例として，通常な圧力分布と，新しい型の圧力分布に対する設計例をも，あわせて示す。

I. Introduction

Progress of computational transonic aerodynamics is remarkable recently. It has become feasible to compute numerically the three-dimensional transonic flow around an full configuration of a realistic aircraft in so far as the flow is governed by the inviscid transonic equations such as the full potential and the Euler equations.[1,2] Viscous effects including the shock-boundary

* Received 28, August, 1985
** The Second Aerodynamics Division

layer interaction and trailing edge separation can be quantitatively evaluated by the time-averaged Navier-Stokes equations for practical design purpose.[3] Viscous airfoil analysis is easily done within a reasonable computing time. Even a three-dimensional transonic flow analysis past a swept wing has become possible as the most advanced vector processor is available.[4]

Meanwhile, progress is not so rapid in the field of developing transonic airfoil and wing design methods. Numerical optimization concept has been investigated in recent years. The number of optimising prameters describing wing geometry, however, becomes too large for practical purpose and computing time required to attain optimized solution will be inpractical. Therefore, ingenuity to use pressure distribution as the optimization parameter has long been cultivated with an abundant harvest.

The conventional design methods are so-called 'inverse method' in which an arbitrary pressure distribution is given and the geometry to realize it is obtained as a solution. Since the geometry is not known beforehand, the pressure distribution is specified as the Dirichlet boundary condition for velocity potential along a presumed geometry. The geometry is modified iteratively until the modified geometry realizes the specified pressure distribution. In such methods, the numerical formulation and flow analysis code must be reformulated so as to satisfy the Dirichlet boundary condition. Iterative inverse methods of this kind have been developed by Carlson,[5] and Tranen[6] for airfoil, Henne[7] for wing, and Shankar[8] for wing-body designs respectively. All of those methods are based on the potential equation. Inverse formulation of the Euler and the Navier-Stokes equations will be difficult.

Another approach to the design method is an iterative "residual-correction procedure" used by Barger and Brooks,[9] Davis[10] and McFadden[11] in their works on the design of a two-dimensional transonic airfoil respectively. Takanashi, one of the present authors, has developed a three-dimensional transonic wing design method based on this approach.[12] In this approach, the geometry correction is made iteratively to compensate for the pressure residual between the specified pressure distribution and a pressure distribution for a presumed geometry obtained by an analysis code. The distinction between each other's methods lies on the difference in the numerical formulation of the geometry correction problem. Takanashi uses a discretized numerical formulation of the three-dimensional transonic integral equation. Takanashi's method has been successfully applied to various wing design for practical purpose using transonic potential flow analysis codes such as Jameson's FLO-22[13] and FLO-27[14] and Boppe's code for wing-body configuration.[15,16] The advantage of present method is that only minimal effort is required in developing the geometry correction code while the analysis code is retained in its original form and can be treated solely as a "black box" to give the pressure distribution for a presumed geometry. As a result, the analysis code can be easily replaced with more advanced code. In the present paper, the concept or the method is extended to apply to any analysis code other than potential code. Then, the method is applied to an analysis code based on the Navier-Stokes equations. Only results for two-dimensional airfoil designs are presented in the paper although the method can be applied to three-dimensional wing design. The results show transonic airfoil designs with shock wave-boundary interaction are easily done. The method is also applicable to low speed airfoil design. Both conventional and unconventional pressure distributions are utilized and presented.

II. Design Methodology

Concept of Design Method

In the following, the logical concept of the present design method is briefly described. The concept needs no rigorous analytical relationship between the geometry and pressure field and it should be considered as qualitative logic. The exact proof and more details are found in the references.[16,17]

Let pressure field P expressed as a function of geometry F, with flow Mach number M_∞, and

Reynolds number Re as parameters in real flow or its flow model, i.e., time-averaged Navier-Stokes equations (abbr. N-S eq.),

$$P = \text{function}\, P\ (F\ ;\ M_\infty, Re) \tag{1}$$

In the design problem, eq. (1) is inverted and geometry F is expressed in terms of P:

$$F = \text{function}\, F\ (P\ ;\ M_\infty, Re) \tag{2}$$

Provided Reynolds number Re is high enough and there exists no separation or separation is weak even if the flow contains shock waves, geometry F can best be approximated by an approximated geometry $\bar{F}$, governed by a sub model; full potential equation, with M_∞ as a parameter.

$$\bar{F} = \bar{F}(P;\ M_\infty) \tag{3}$$

then, geometry F is expressed as:

$$F = \bar{F} + \delta R \tag{4}$$

where R represents all of the higher order terms and δ is a coefficient smaller enough than unity; $|\delta| \ll 1$.

Function F may be a nonlinear function but it can be considered to be a continuous function of P, M_∞ and Re at least locally in practical stand point of view. For a small perturbation of pressure field, ΔP, geometry is perturbed as ΔF from the original geometry, F_0 , and the new geometry, F_{target}, is expressed as:

$$F_{target} = F_0 + \Delta F_0 \tag{5}$$

where Δ represents small perturbation and subscript $_0$ represents original value, respectively. The exact relation eq.(4) is brought into the second term of eq.(5), obtaining;

$$\begin{aligned} F_{target} &= F_0 + (\Delta \bar{F}_0 + \Delta\ (\delta R_0)) \\ &= F_0 + \Delta \bar{F}_0 + \delta \Delta R_0 \end{aligned} \tag{6}$$

Under the present assumptions, perturbation of all of the higher terms ΔR_0 is small enough to be expressed as

$$\Delta R_0 = \epsilon R_0,\ |\epsilon| \ll 1 \tag{7}$$

Therefore, equation (8) holds.

$$F_{target} = F_0 + \Delta \bar{F}_0 + \delta \epsilon R_0 \tag{8}$$

As δ and ϵ are negligibly small, the primary part of perturbation is $\Delta \bar{F}_0 \cdot F_{target}$ can best be approximated by,

$$F_{target} \doteq F_0 + \Delta \bar{F}_0 \tag{9}$$

The significant feature of Takanashi's method is that only the perturbation term or the geometry correction term in other words, $\Delta \bar{F}_0$, is given by an approximated sub-model while the original geometry F_0 as well as P can be expressed by any flow model governed by eq.(1) such as full potential, Euler, N-S equations and even wind tunnel experiment and flight testing. In the present paper, N-S equations are used.

Geometry Correction Problem

The derivation of the integral equation formulation for the geometry correction problem is described in reference.[12] And the summary is presented only. The three-dimensional full potential equation is written in terms of perturbation velocity potential ϕ . Assume a solution ϕ for an initial presumed wing geometry has been obtained by means of an existing flow analysis code, eq.(1). If a perturbation $\Delta\phi$ from the known solution ϕ is introduced, the governing equation is expressed in terms of unknown $\Delta\phi$ and known solution ϕ with the flow tangency condition and boundary condition on pressure distribution on the wing surface. The geometry correction equation $\Delta\bar{F}_0$ in terms of $\Delta\phi$ is obtained under a good reasonable assumption of neglecting higher order terms. Applying Green's theorem, the perturbed equation is converted into an integro-differential equation. After a little analytic manipulations and applying a decay function in normal direction to wing surface, the equation reduces to a simple two-dimensional integral equation for wing surface. The unique solution is obtained with trailing edge closure condition enforced. The present closure condition means that the correction of the trailing edge thickness is zero,i.e.,the trailing edge thickness of the original wing remains unchanged. The original trailing edge thickness, itself, need not be zero. This condition, however, does not necessarily mean that the resulting wing

section contour has no crossing of the upper and the lower surfaces along the chord from the leading edge to the trailing edge. Such a crossing if occurs does not give physically reasonable wing and the specified pressure distribution must inevitably be modified in order to obtain a physically reasonable wing. The analysis code must be the one which overcomes the resulting mapping trouble between the physical and computational spaces.

Within the assumption in the present paper, $\Delta \bar{F}_0$ remains continuous for a pressure field perturbation containing discontinuity such as shock waves provided the shock wave is approximated as normal shock wave to wing surface. More precisely, slope, $\Delta(d\bar{F}_0 / dx)$, is proportional to Δ w, velocity perturbation correction normal to the surface and it remains constant across the shock wave.

A discretized numerical formulation is formulated to approximate the integral equation and the resulting linear system is solved easily by standard techniques such as the Gaussian elimination method.

Navier-Stokes Solver

N-S equations are used as the flow solver eq.(1). One of the purpose of the present paper is to show that Takanashi's method can be applied to N-S flow solver as well as the full potential flow solvers.

Three-dimensional N-S flow solver for a practical transonic swept wing is recently developed as a research code at National Aerospace Laboratory[4]. The computing time required is prohibitively large for the present purpose since the flow solver must be run repeatedly several times. Instead, two-dimensional airfoil analysis code, NSFOIL, [18] is used here and the transonic airfoil design is attempted in place of the wing design. Two-dimensional formulation of the geometry correction problem is straight forward reduction of the previous section and is omitted here. There is no other reason to circumvent the three-dimensional trial theoretically.

Flow solver, NSFOIL, is based on the Implicit Approximate Factorization scheme for N-S eq. originally developed by Beam, Warming[19] and Steger.[20] The treatment of internal boundary on the airfoil surface and wake boundary is improved to be treated implicitly in the formulation of block-tri-diagonal formulation. Also, time step width is given as a monotonically increasing hyperbolic tangent function of iteration step number. The initial time step width is 2^{-p} and increased upto 2^{-q} , then kept constant thereafter. The values of p and q are specified arbitrarily. p = 18 and q = 6 gives stable computation for most ranges of free stream Mach number, angle of attack and practical Reynolds number. p was chosen to satisfy Courant number less than unity and q is limitted by the nonlinear stability and physical scale of time. For transonic buffet computation, q will be reduced to 7 or 8 to make computation stable. It is important time step width asymptotically increased to the final time step width 2^{-q}. Abrupt change of time step width leads to instability. The present methods is quite robust when used as a practical aerodynamic design tool.

The code has been extensively applied to the analysis of various supercritical airfoils at wide ranges of Mach number, angle of attack and Reynolds number without any trouble such as the divergence of computation and compared with the experimental results by the High Reynolds Number Two-Dimensional Transonic Wind Tunnel at NAL[3,21].

The mesh system used by NSFOIL is generated by a body-fitted mesh generation code, AFMESH.[22] Various combinations of mesh generating methods such as Laplace and Poisson equation methods, geometric construction method, and algebraic sheared mesh generation method are incorporated along with many options to serve the designer's request. The user can easily generate any specific mesh around airfoil.

Procedure of design

The flow chart of design procedure is shown in Fig.1. In the present paper, the combination of AFMESH and NSFOIL is used as the 'ANALYSIS' code in the chart and wing design code in the previous paper[12] is used as the

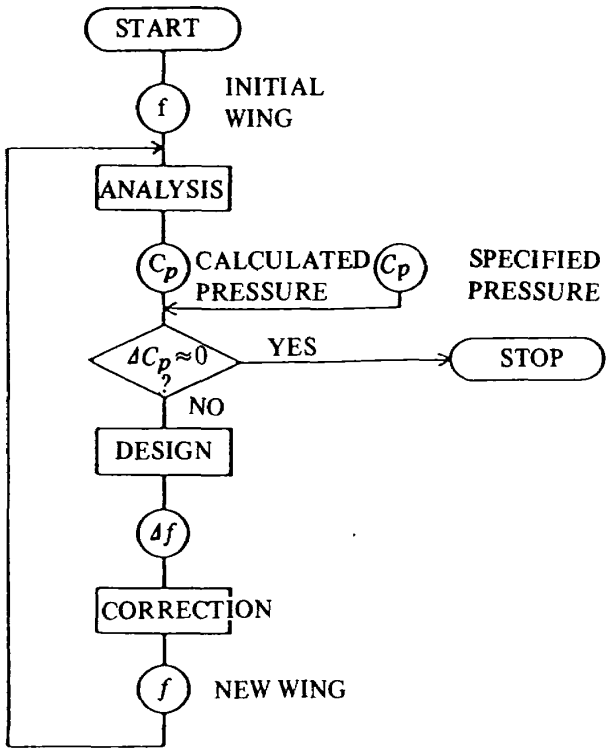

Fig. 1 Flow chart of design procedure.

'DESIGN' code. For 2-D airfoil design, a rectangular wing of high aspect ratio of 20 was used with the same pressure distribution and wing section geometry as the ones given by two-dimensional NSFOIL analysis code. Direct application of 3-D wing design code does never hamper the validity of the methods and the computed results for airfoil design.

A design system Transonic Full Potential Design based on Navier-Stokes equations (TFPDNS) was constructed and the each step of the iterative computation of analysis and design modes is handled on a TSS terminal although the analysis code has to be run as a batch job due to its computing time required. Computing times for the rest of the jobs including data handlings are negligibly small.

III. Computed Results

Case I. Shockless Airfoil Design

To demonstrate the practical applicability of the present procedure, some of the computed results are presented for transonic and low speed airfoil designs.

The first example is obtained to realize a shockless supercritical pressure distribution with lift coefficient C_L = 0.6 starting from an airfoil geometry with a pressure distribution containing a strong shock wave. A computed pressure distribution obtained by NSFOIL was used as the shockless target pressure distribution. The basic airoil geometry is the same one which gave the target pressure distribution but at a different angle of attack.

Garabedian-Korn airfoil 75-06-12 of thickness to chord length ratio of 12% was selected at its design condition of the flow Mach number, M_∞ = 0.75 and the angle of attack, α = 0.8 degrees, as the target. The Reynolds number $Re = 1.3 \times 10^7$. The computed flow field is a shockless flow field. Turbulent boundary layer is calculated by Baldwin-Lomax algebraic turbulence model with transition included. No upwind differencing was used. Impulsive start condition was applied. Computing mesh consists of 125 x 51 C-type grid with 93 points on airfoil surface (47 points on each side). The first mesh spacing adjacent to the surface is 0.00001 of chord length and corresponds to y^+ less than unity. The outer boundary is placed at 12 chord length away from the airfoil. Total time step number of 5000 were required to reach converged flow field for one analysis mode.

The basic flow field was calculated at angle of attack α = 2.0 degrees. The flow contains strong shock wave on the upper surfae. During the design procedure, the angle of attack in the analysis mode is fixed to α = 2.0 and the space coordinates (x, y) are also fixed. All of the other computational parameters for NSFOIL and AFMESH are fixed same as that of the initial flow analysis mode. Only the coordinates of the geometry corrected by the design mode was replaced with the new one. The mesh was constructed around the new geometry to serve the N-S analysis.

The history of lift coefficient C_L at each mode is shown in Fig.2 . The major change of C_L is accomplished in the early few modes. the iterative procedure showed the geometry corrected at each design mode rotates in the fixed space without significant distortion of geometry

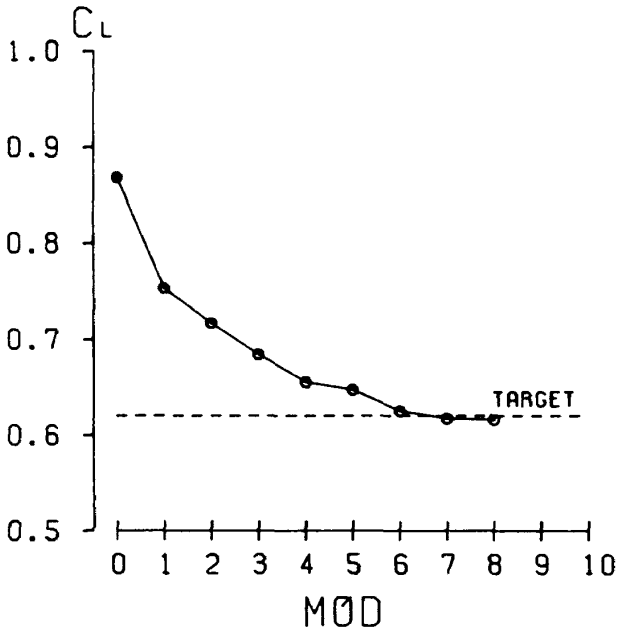

Fig. 2 History of lift coefficient, Case I.

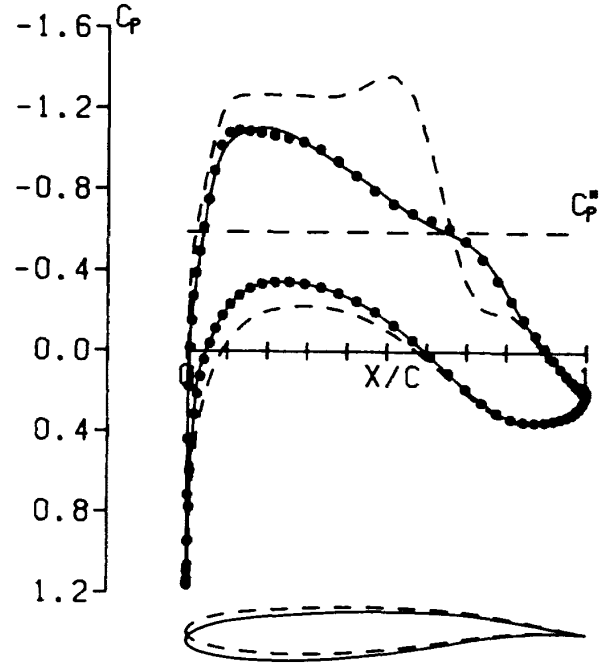

Fig. 3 Comparison of pressure distributions and geometries between designed (solid line), basic (dashed line) and target (dotted line), Case I.

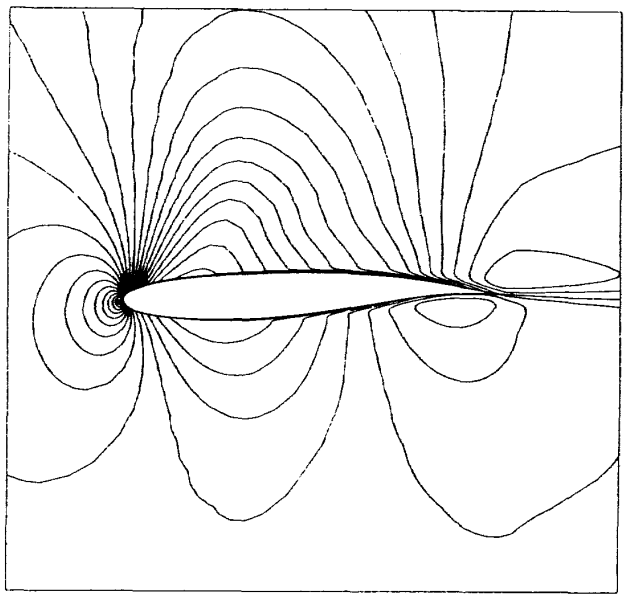

a) density field

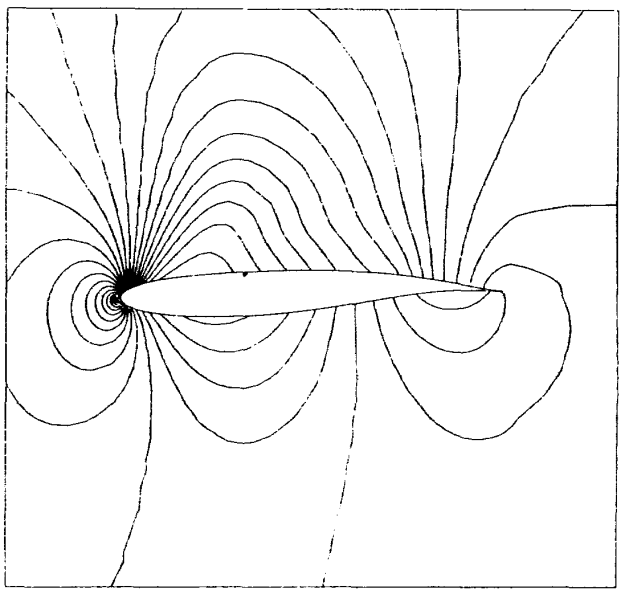

b) pressure field

Fig. 4 Flow field around the designed airfoil, Case I.

itself. In Fig.3, the designed pressure distribution (symbol •) as well as the original pressure distribution (dashed line). The corresponding geometries are also compared in the same figure with the same lines as for pressure, respectively. The final designed geometry precisely coincided with the original airfoil geometry with the rotated angle of attack – 1.2 degrees corresponding to the difference between the fixed angle of attack 2.0 degrees and the target angle of attack 0.8 degrees in fixed original space coordinates.

In Fig.4, density and pressure fields around the designed airfoil are presented. To understand how the correction proceeds, the iterative history of design is depicted in Fig.5. The corresponding geometries are also compared in the same figure. The dashed line represents the basic geometry and the soild line represents designed geometry, respectively. The scale is exaggerated in normal direction to illustrate the

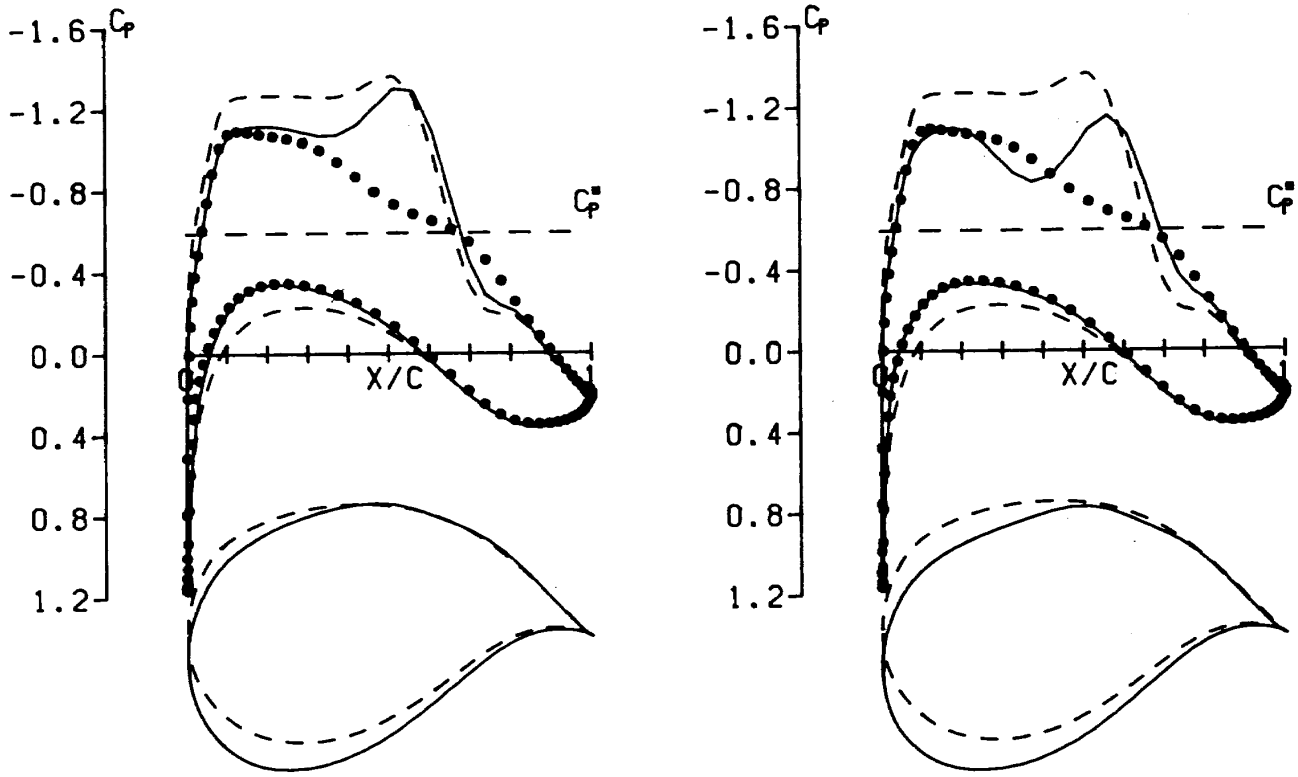

a) mode 1

c) mode 3

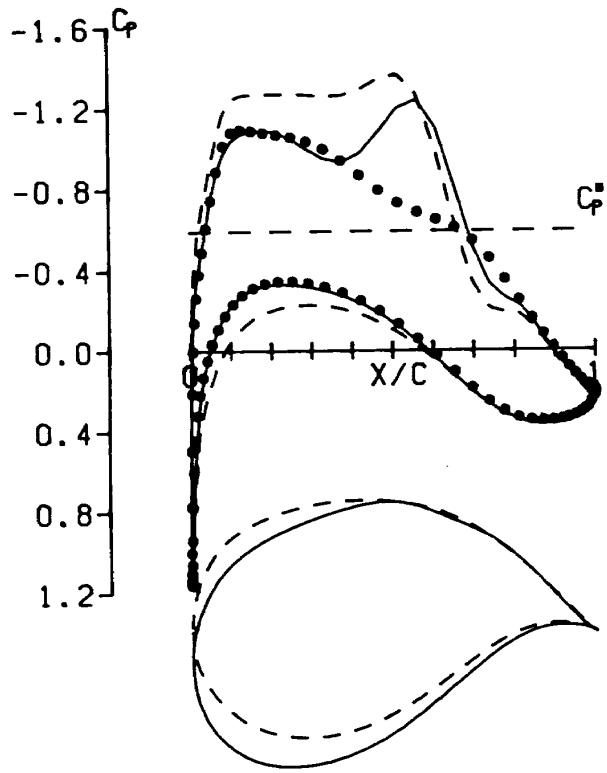

b) mode 2

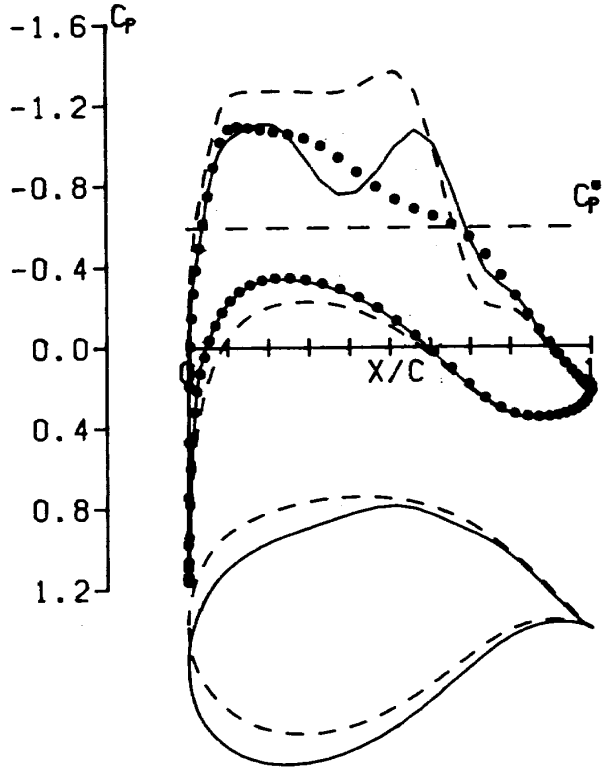

d) mode 4

Fig. 5 Iterative history of design and pressure recovery, Case I.

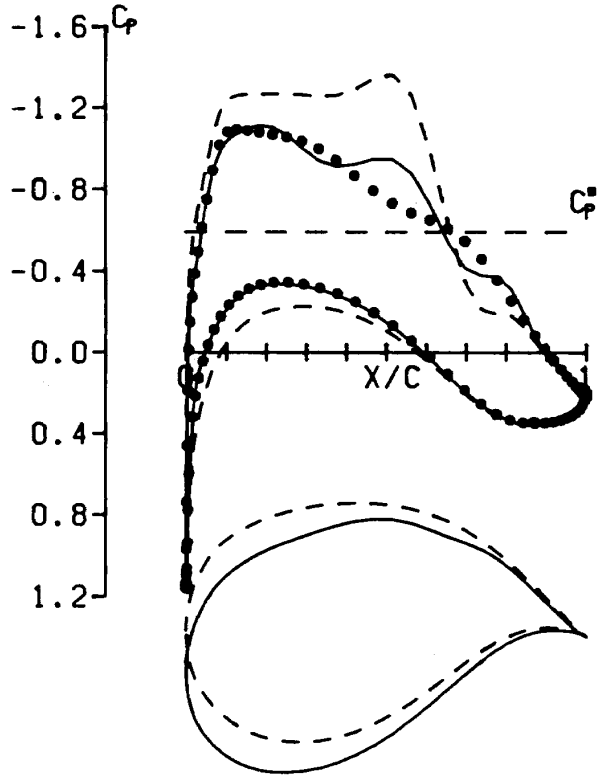

e) mode 5

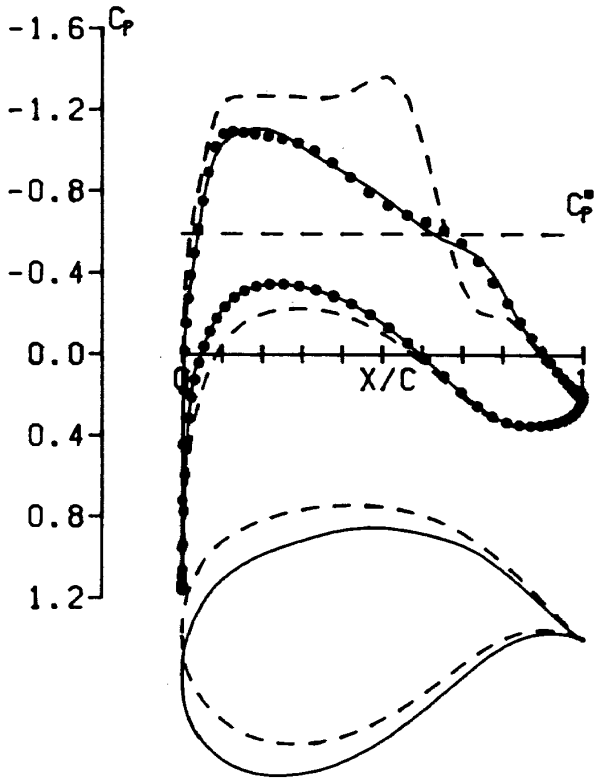

g) mode 7

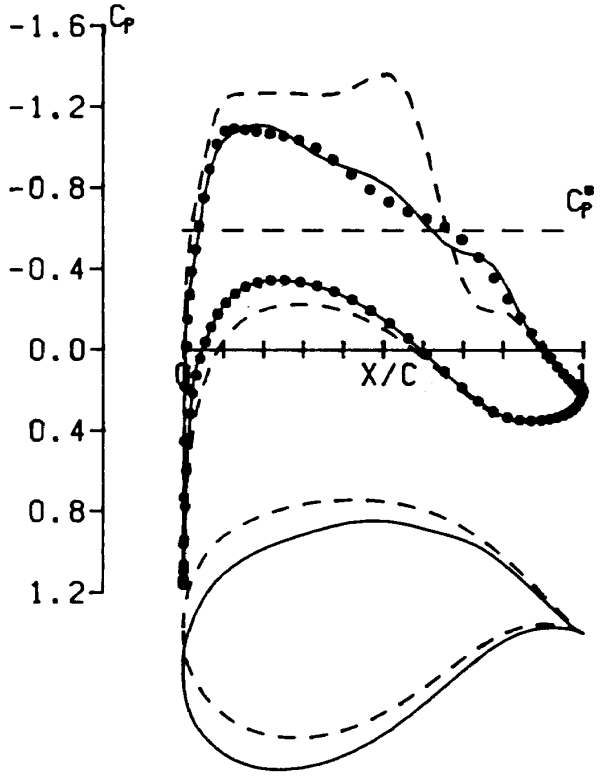

f) mode 6

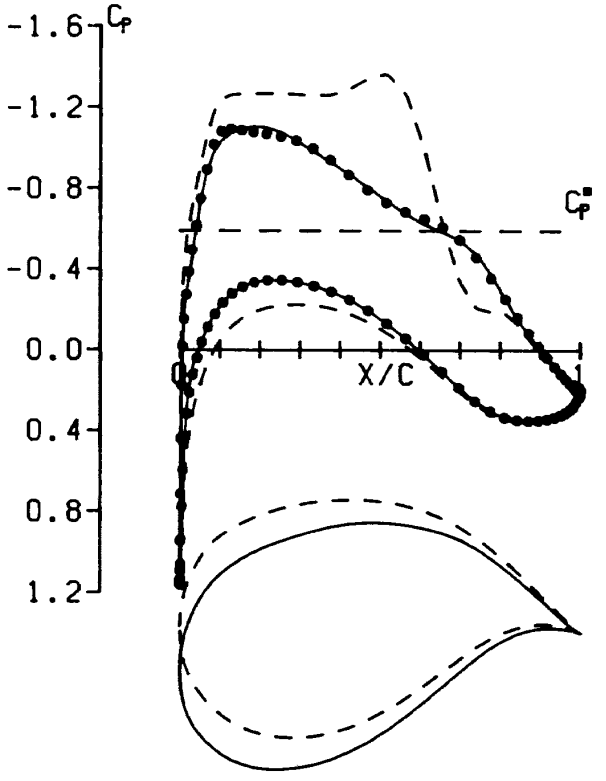

h) mode 8

Fig. 5 Continued.

correction of geometry. It is clear that the lower surface pressure distribution where the flow is subcritical, converges with only one iteration. The upper surface peak pressure behind the leading edge expansion also converges with one iteration. The pressure correction near the shock wave requires several iterative steps to attain the target pressure. The convergence is obtained oscilatorily in the intermediate steps until shock wave disappears finally.

In Fig.6 local Mach number distributions around the original airfoil and the designed airfoil are compared. Strong shock wave on the upper surface of the original airfoil disappears on the designed airfoil. The boundary layer characteristics such as the displacement thickness, momentum thickness and form factor are computed, although not shown here to save space. As the shock wave does not exist, these characteristics are moderate compared with the original ones at the basic condition. Boundary layer growth behind the shock wave seen in Fig.6(a) is improved in the designed airfoil as shown in (b).

The resolution of flow field especially such as the shock wave and boundary layer in N-S solver depends on the total mesh numbers available. In the present case 47 points are distributed on one side of the surfaces. The spacing near the shock in flow direction is rather coarse. The shockless pressure distribution in this case means the one which is attainable within the present analysis resolution. The accomplishment of design target should be measured within the resolution of utilized analysis code and applied mesh numbers. In fact, the present airfoil was tested at NAL wind tunnel and weak shock wave exists at the present condition. The adaption of more refined mesh or solution adaptive grid for shock wave will give a flow with shock wave. Shockless design can be sought easily in such trial and such extension is in progress.

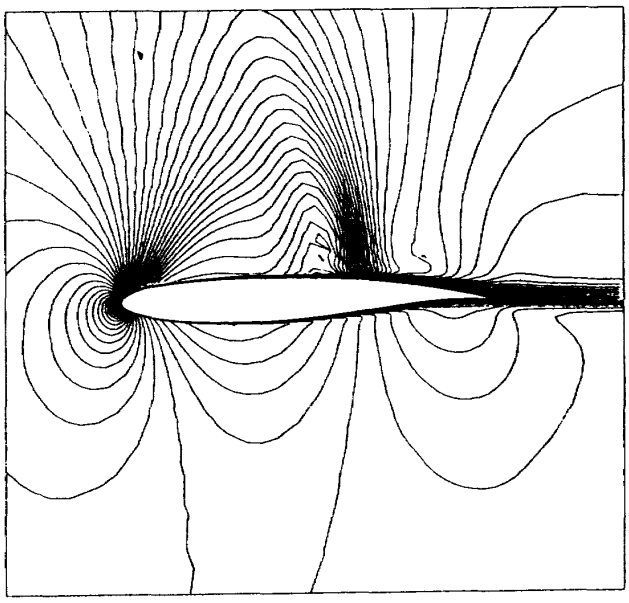

a) basic airfoil

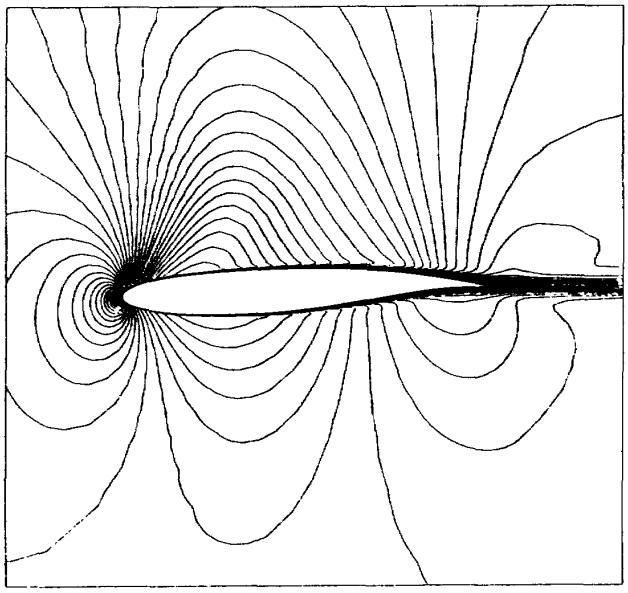

b) designed airfoil

Fig. 6 Comparison of local Mach number distributions.

Case II. Supercritical Airfoil Design

Case I was to design the known target which is a computed result by the same analysis code. One may suspects the validity of the present design procedure on the case of arbitrarily specified pressure distribution. To prove this, another case was designed for a rooftop supercritical pressure distribution with the lift coefficient of C_L=0.7. The upper surface pressure distribution was arbitrarily specified this time while the lower surface pressure distribution was the same one as that of the case I. Target geometry is not known beforehand. The flow Mach number, Reynolds number and other parameters were set same as in the Case I. Solution for airfoil GK-75-06-12 at the angle of attack of 0.8 degrees, the design point and the previous

target point in the previous case, was used as the basic airfoil geometry and the basic pressure field.

To accelerate the convergence of the analysis code, the distribution of flow variables in the initial flow field at each analysis mode was assumed to be the same one as that of the converged solution of the previous analysis mode instead of using the conventional impulsive start condition. Since the modification of the geometry is small at each one design mode, the resulting flow field does not differ from the solution of the previous mode too much in this case. This initial flow field condition option incorporated in code NSFOIL reduced the computing time less than a half compared with the impulsively started computation case. This, however, is not always the case since there is no guaranty that the amount of correction of geometry is small enough that the flow field solution distance in the topological solution space is also small. Such cases have been encountered often in the other design examples and led to divergence of computation.

Only two iterations gave almost satisfactory result of attaining the lift coefficient of C_L=0.69. No more than four iterations were needed to reach the target. The iterative history of the pressure distribution and the geometry modifications at the each design mode is shown in Fig. 7 (a) to (d). The same symbols and lines as in Fig. 3 are used to identify the target, the designed and the basic distributions and geometries. The history of the lift coefficient is shown in Fig. 8. The designed geometry and its pressure distribution compared with the target and the basic ones are illustrated in Fig. 9. It can be seen that the designed geometry has the thicker thickness and the larger camber distribution than those of the basic airfoil. The attained pressure distribution can be considered shockless within the present resolution of the analysis code. There is the trailing edge separation of the boundary layer beginning at 98 per cent chord station on the upper surface while the basic profile has no separation. The existence of separation of the boundary layer, however, does not preclude the

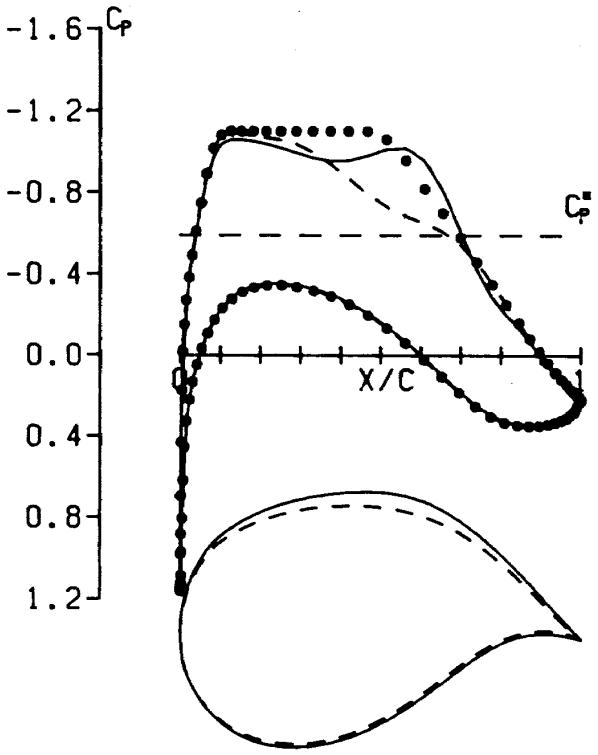

a) mode 1

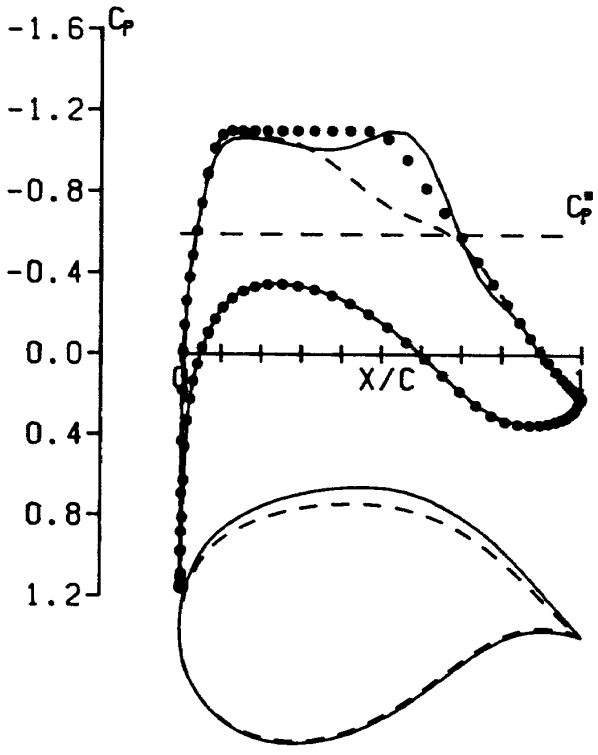

b) mode 2

Fig. 7 Iterative history of design and pressure recovery, Case II.

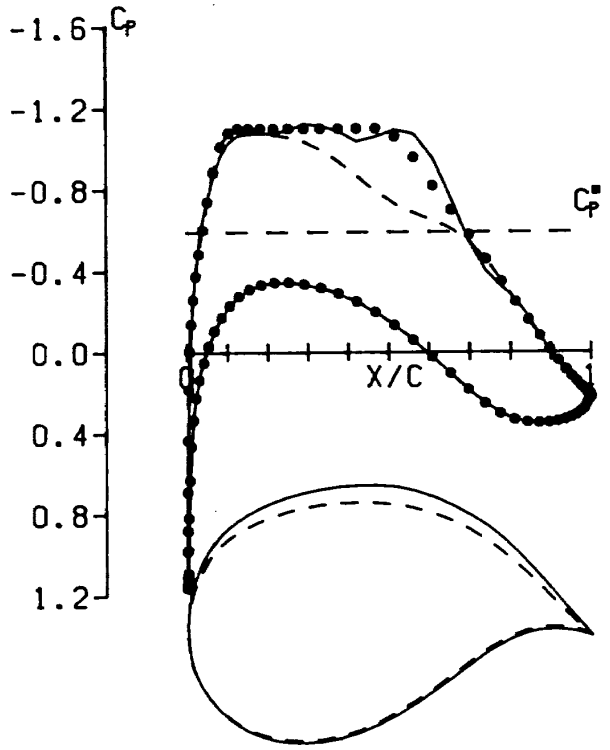

c) mode 3

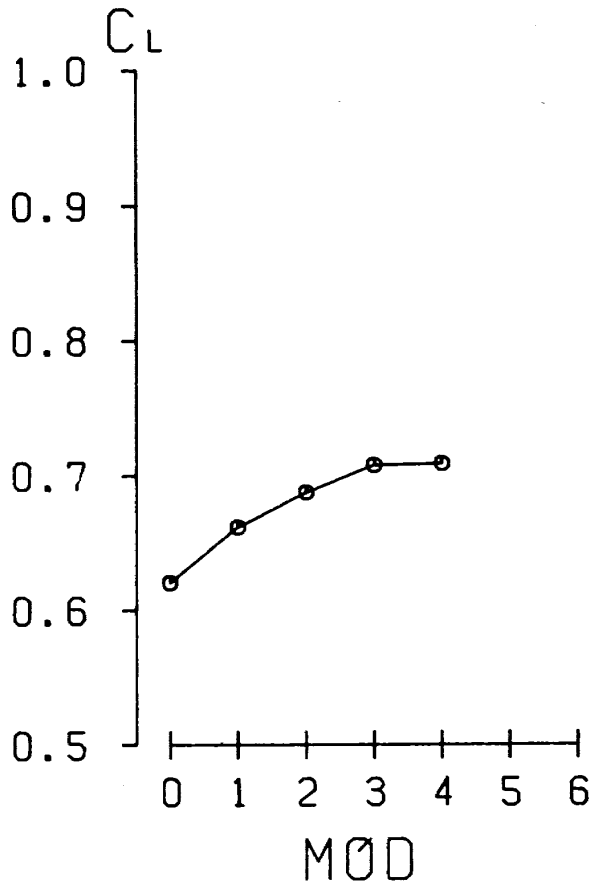

Fig. 8 History of lift coefficient, Case II.

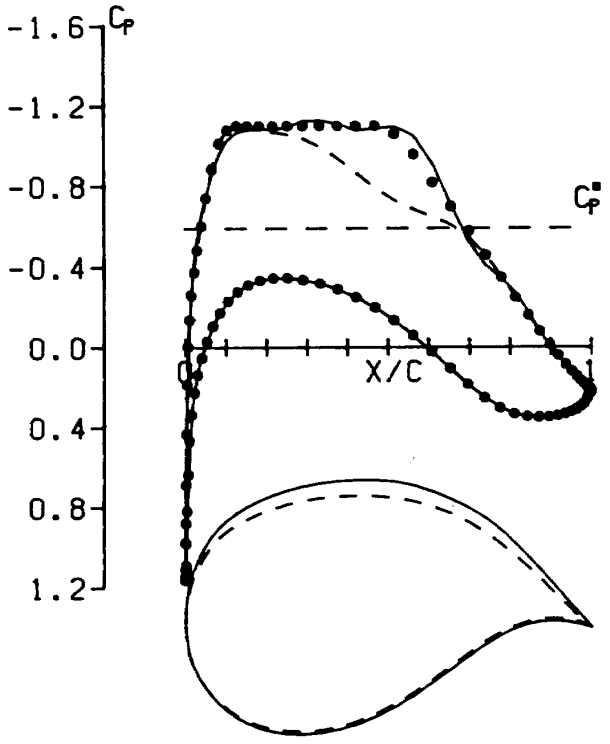

d) mode 4

Fig. 7 Continued.

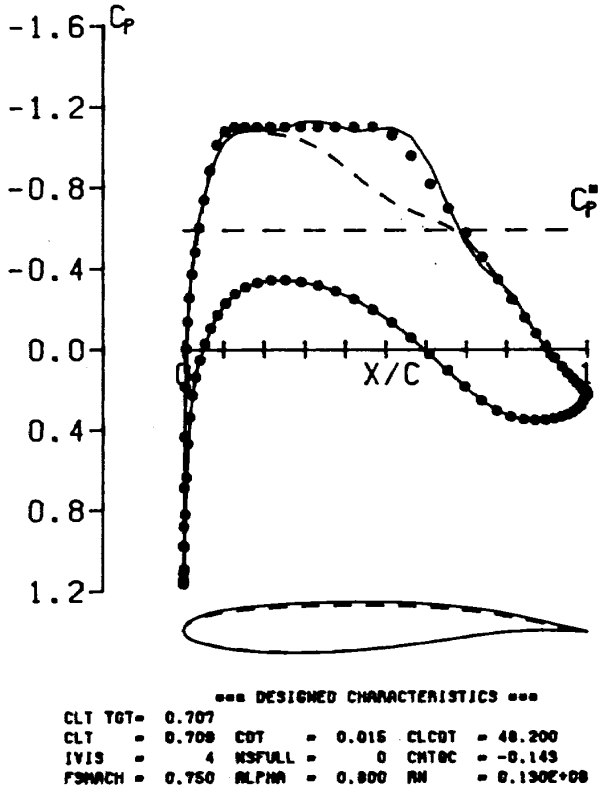

*** DESIGNED CHARACTERISTICS ***

CLT TGT=	0.707				
CLT =	0.709	CDT =	0.015	CLCDT =	48.200
IVIS =	4	NSFULL =	0	CMTOC =	-0.143
FSMACH =	0.750	ALPHA =	0.800	RN =	0.130E+08

Fig. 9 Comparison of pressure distributions and geometries between designed and basic ones, Case II.

present procedure to apply.

Case III. Arbitrarily Specified Design

In case III, pressure distribution along the fore part of the airfoil including leading edge region was specified arbitrarily as depicted as dotted line in Fig. 10. The design target of the lift coefficient C_L is 0.62. The basic airfoil and pressure distribution used is the same one used in the previous case.

The convergence required ten design modes. The iterative history of the lift coefficient, C_L does not indicate proper evaluation of the design convergence since the basic pressure distribution gives the same value of the lift coefficient. The lift coefficient remains almost constant during the iterations. The pressure distribution, however, is improved at each mode to approach the specified pressure profile. The pressure profile on lower surfase beyond 2.5 per cent chord station recovered with only two design modes. The leading edge region required a few more design modes to approach to the target pressure distribution. The upper surface pressure profile exhibits sinusoidal oscillation along chort and its amplitude gradually decreases as design mode proceeds. At mode 10 the pressure recovery to the target pressure distribution is almost satisfactory in practical point of view although a sharp oscillation of pressure still remains near the leading edge. It is conjectured that purely arbitrary specification of the pressure profile is the major reason why many iteration steps are required. Such a profile might be ill-posed one and the numerical solutions of the analysis and design codes governed by numerical parameters including mesh spacing and smoothing coefficients may not give such a distribution. Even if such is not the case, the similar situation may arise. The result of mode 10 is considered as converged solution under the present circumstances.

The basic airfoil GK-75-06-12 has cusp type trailing edge of zero thickness. During the iterations, physical ill-posedness did occur. Thickness became negative in the region near the trailing edge. A trailing edge thickness modification was

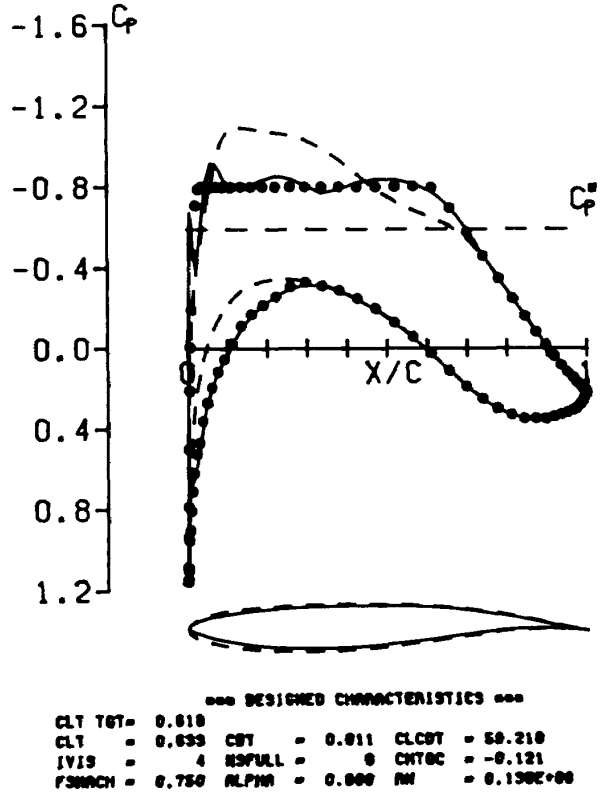

Fig. 10 Comparison of pressure distribution of designed airfoil at mode 10, Case III.

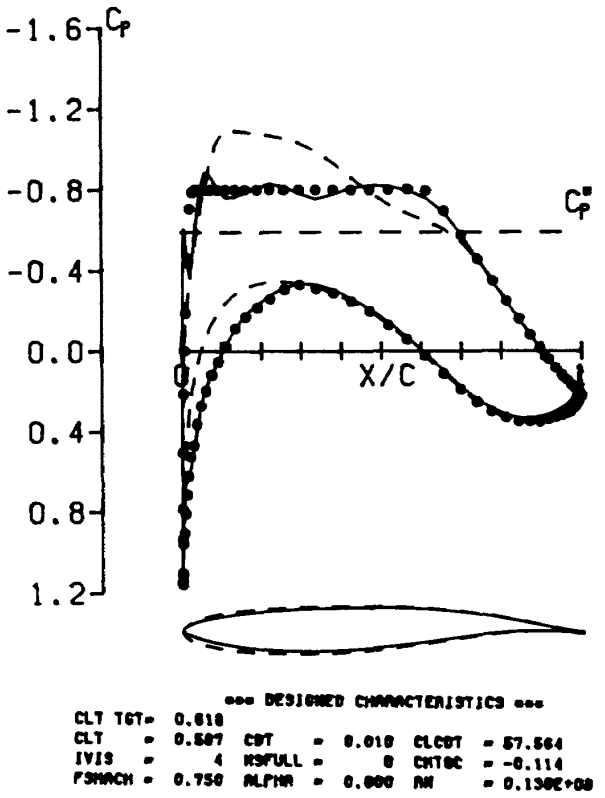

Fig. 11 Pressure distribution of trailing edge modified airfoil at mode 10A, Case III.

adopted to the airfoil geometry designed at mode 10. Trailing edge thickness δ_{TE} was enlarged from zero to 0.0025 of chord length. Local thickness distribution correction proportional to $\delta_{TE} \cdot \sqrt{x}$ was evenly added to the both sides of surfaces from leading edge to trailing edge. Flow analysis was made for the modified geometry and its pressure profile is shown in Fig. 11. Pressure profile remain unchanged except the trailing edge region where small discrepancy appeared due to the modification. The loss of the life coefficient due to this geometry modification is 0.036 and this is recovered by the increment of angle of attack of 0.12 degrees without the change of the pressure profile and the value of the drag confficient.

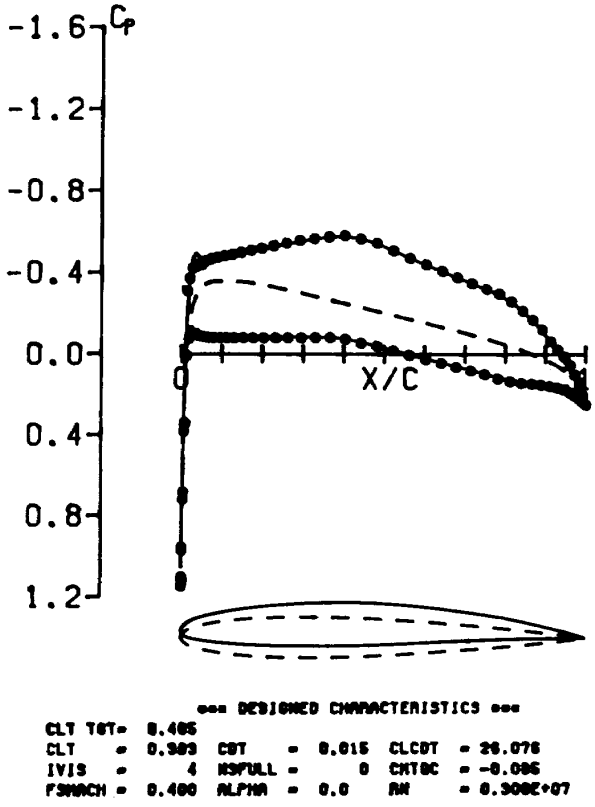

Fig. 12 Pressure distribution of designed airfoil at mode 3, Case IV.

Case IV. Conventional Low Speed Airfoil Design

A conventional low speed airfoil design is presented to show the applicability of the present method. An arbitrary pressure distribution similar to the one of NACA 64 series with the lift coefficient of C_L=0.4 was specified. Flow condition is; the flow Mach number, M_∞=0.40, the angle of attack, α=0° and the Reynolds number, Re=3x10^6. Other parameters remain the same as in the previous cases. The computing mesh consists of 113x33 grids with 93 points on airfoil surface. The computing region extends only 2 chord length in x and y directions from airfoil. Mesh distribution in the vicinity of airfoil is similar to that of the previous cases. The effects of outer boundary position is small and can be compensated by other analytic means for low speed design if necessary. The mesh spacing along surface at the leading edge was 0.0025 chord length to properly evaluate the detail of curvature distribution in the leading edge region.

NACA 0010 at zero angle of attack was chosen as the basic airfoil. After 3 design modes the pressure recovery was satisfactorily accomplished with the lift coefficient of C_L=0.393 as shown in Fig. 12. The final airfoil has maximum thickness to chord ratio of 0.11 and the geometry contour is similar to a canventional NACA 64 series airfoil. From this result, it can be said that the conventional low speed airfoil design can be done quite easily.

Case V. Unconventional Low Speed Airfoil Design

Another example of the low speed design is a thick airfoil with rear loading pressure profile with the lift coefficient of C_L=0.6. Flow condition is; the flow Mach number, M_∞=0.4, the angle of attack, α=0°, and the Reynolds number, Re=6x10^6. Computing region extends 4 chord length in both of x and y directions from the airfoil. Geometry of the airfoil NACA 0024 at the angle of attack, α=0 was used as the starting geometry.

The result is shown in Fig. 13. The basic airfoil has weak trailing edge separation of the boundary layer. As the iteration of the design proceeds, the life coefficient of C_L=0.56 was attained at mode 3 with the excellent pressure recovery except the region of last 30 per cent of the chord on the lower surface where rear loading requirement is severe. At 65 per cent chord station on the lower surface a weak

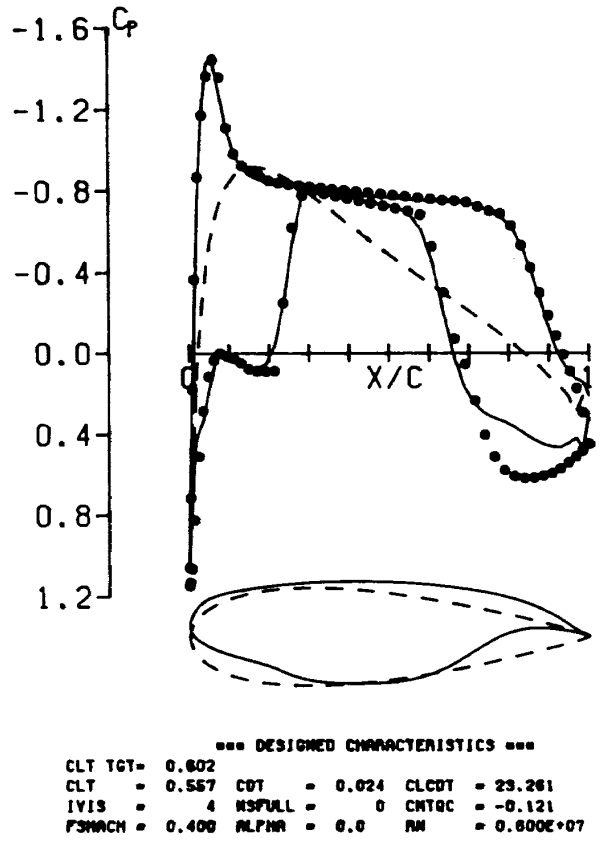

Fig. 13 Pressure distribution of designed airfoil with trailing edge modification at mode 3A, Case V.

separation of the boundary layer occurs. Further advancement of iteration mode is needed to recover the pressure difference at this rear loading region, but it resulted in the formation of an extraordinary large concavity on the lower surface crossing the upper surface, and yet the pressure was not recovered. The close examination of the flow field shows existence of a larger reverse flow starting at 65 per cent chord station. For such a large separation existing, the assumption underlying the present design methodology may become invalid.

The converged flow field of previous mode was used as the initial condition for the next analysis mode in both of Case IV and V to reduce the computing time.

The examination of design mode 3 shows geometry has very small crossing of the surfaces in front of trailling edge. To obtain physically reasonable geometry, the trailing edge modification was made with δ_{TE}=0.0020 without lift loss. The pressure profile and the geometry in Fig. 13 is for this modified airfoil. The maximum thickness to chord ratio obtained is 0.255.

The present rear loading pressure profile is too severe to design and we conjecture there may exist no physically reasonable geometry to correspond. The pressure profile should be modified to more moderate one if any reasonable geometry is wanted.

IV. Computing Resources

Computing time for analysis code depends on the size of mesh, scale of computing region and convergence criterion. A standard analysis mode in Case I required about 110 minutes on FACOM M-380 (9 MFLOPS machine) installed at National Aerospace Laboratory. The design code and mesh generator code require less than one minute to run. Therefore the total computing time is governed by the analysis code requirement. Case I required total of 16 hours. Case II was achieved with four hours with the improved initial condition. Low speed cases were done far less hours.

Memory size requirement is easy one. The analysis code requires about 4 Mega Bytes of memory and the design code requires negligibly small size.

NAL is requesting fund to install Numerical Simulator; a super-computer with performance of more than one Giga FLOPS in next fiscal year. Reduction of 50 times of the present computing time is expected in vector processing. If such a case, one design of airfoil can be done in less than 5 minutes. Even the three-dimentional wing design using Navier-Stokes code will become possible in practice.

V. Concluding Remarks

A practical and flexible procedure of transonic airfoil design based on the Navier-Stokes equations is proposed, and examples including low speed design are demonstrated as effective. The inherent difficulty concerning the specification of pressure distribution near the trailling edge in the conventional potential design codes with the outer potential flow-turbulent boundary

layer interactive formulation is excluded in the present formulation. Shock-boundary layer interaction and trailing edge separation is incorporated automatically because the Navier-Stokes equations are used.

The ill-posedness of the inverse problem for geometry design may not be avoidable even in the present method. In the practical design, however, the method tries to find out an approximate solution, *i.e.*, geometry, which lies in the vicinity of the basic geometry upon which the flow analysis, *i.e.*, the direct problem is solved in the analysis mode. Each one of transient iterative mode has its logical validity upon this. Even an approximate solution will suffice for the practical purpose when we consider the fact that the Navier-Stokes solver or even the wind tunel testing is only an approximation to the actual flight of aircraft.

The methodology can apply to three-dimensional wing. Only the requirement of computer resources prohibits its demonstration. Applications to the Euler codes, 3-D Navier-Stokes codes and the other flow regimes such as the cascade flow are now in progress and will be reported in near future.

A part of the contents of paper was presented in References 23 and 24.

References

1. Boppe, C.W. and Stern, M.A., "Simulated Transonic Flow for Aircraft with Nacelles, Pylons, and Winglets," AIAA Paper 80–0130, 1980.
2. Jameson, A. and Baker, T.J., "Solution of the Euler Equations for Complex Configurations," AIAA Paper 83–1929, 1983.
3. Miyakawa, J. and Hirose, N., "The Comparison of the Transonic Airfoil Calculation by NSFOIL with the Wind Tunnel Test Data at High Reynolds Number," Proc. 2nd NAL Symp. on Aircraft Computational Aerodynamics, NAL SP-3, 245–254, 1984.
4. Obayashi, S. and Fujii, K., "Computation of Three-Dimensional Viscous Transonic Flows with the LU Factored Scheme," AIAA Paper 85–1510-CP, 1985.
5. Carlson, L.A., "Transonic Airfoil Design Using Cartesian Coordinates," NASA CR-2578, 1976.
6. Tranen, T.L., "A Rapid Computer Aided Transonic Airfoil Design Method, "AIAA Paper 74–501, 1974.
7. Henne, P.A., "Inverse Transonic Wing Design Method," J. of Aircraft, **18**, 121–127, 1981.
8. Shanker, V., "A Full Potential Inverse Method Based on a Density Linearization Scheme for Wing Design," AIAA Paper 81–1234, 1981.
9. Barger, R.L. and Brooks, C.W., "A Streamline Curvature Method for Design of Supercritical and Subcritical Airfoils," NASA TN D-7770, 1974.
10. Davis, W.H. Jr., "Technique for Developing Design Tools from the Analysis Methods of Computational Aerodynamics," AIAA Paper 79–1529, 1979.
11. McFadden, G.B., "An Artificial Viscosity Method for the Design of Supercritical Airfoils," Ph. D. Thesis, New York University, New York, 1979.
12. Takanashi, S., "Iterative Three-Dimentional Transonic Wing Design Using Integral Equations," J. Aircraft, **22**, 655–660, 1985 / AIAA Paper 84–2155, 1984.
13. Jameson, A. and Caughey, D.A., "Numerical Calculation of the Transonic Flow Past a Swept Wing," NASA CR-153297 (COO-3077-140), 1977.
14. Jameson, A. and Caughey, D.A., "A Finite Volume Method for Transonic Potential Flow Calculations," AIAA Paper 77–635, 1977.
15. Boppe, C.W. "Transonic Flow Field Analysis for Wing-Fuselage Configurations," NASA CR-3243, 1980.
16. Takanashi, S., "Transonic Wing and Airfoil Designs Using Inverse Code WINDES," Proc. 3rd NAL Symp. on Aircraft Computational Aerodynamics, June, 1985, NAL SP-5, 251–256, 1985.
17. Takanashi, S., "Logical Concept of Transonic Wing Design Code WINDES," NAL-TR to

be published.

18. Kawai, N. and Hirose, N., "Development of the Code NSFOIL for Analizing High Reynolds Number Transonic Flow around an Airfoil," NAL TR-816, 1984.
19. Beam. R. and Warming, R.F., "An Implicit Finite-Difference Algorithm for Hyperbolic Systems in Conservation Law Form," J. Comput. Phys., 22, 87–110, 1976.
20. Steger, J.L., "Implicit Finite Difference Simulation of Flow About Arbitrary Geometries with Application to Airfoils," AIAA Paper 77–665, 1977.
21. Hirose, N., Kawai, N., Oguchi, K. and Kodera, T., "Validation and Comparison with Experiment of a High Reynolds Number Transonic Flow Airfoil Analysis Code NSFOIL," Proc. 2nd NAL Symp. on Aircraft Computational Aerodynamics, NAL SP-3, 235–244, 1984.
22. Hirose, N., Kawai, N., Isawa, T., and Kikuchi, M., "Development of Grid Generator Code AFMESH for Transonic Airfoil Analysis Codes," Proc. 13th Ann. Meeting, Jap. Soc. Aero. & Space Sci., 158–161, 1982.
23. Hirose, N., Takanashi, S. and Kawai, N., "Transonic Airfoil Design Based on Navier-Stokes Equations to Attain Arbitrarily Specified Pressure Distribution-an Iterative Procedure," presented at the AIAA 18th Fluid Dynamics and Plasmadynamics and Lasers Conference, Cincinnati, Ohio, July 15–18, 1985, AIAA Paper 85–1592, 1985.
24. Hirose, N., Takanashi, S. and Kawai, N., "Transonic Airfoil Design Based on Navier-Stokes Equations to Attain Arbitrarily Specified Pressure Distribution-an Iterative Procedure," presented at the Ann. Meeting of the Jap. Soc. Aero. & Space Sci. held at Tokyo, Japan, April 2–4, 1985.

TECHNICAL REPORT OF NATIONAL
AEROSPACE LABORATORY
TR-901T

航空宇宙技術研究所報告901T号(欧文)

昭和61年3月発行

発行所 航空宇宙技術研究所
東京都調布市深大寺東町7－44－1
電話武蔵野三鷹(0422)47-5911(大代表)〒182
印刷所 株式会社 共進
東京都杉並区久我山5－6－17

Published by
NATIONAL AEROSPACE LABORATORY
7-44-1 Jindaiji higashi, Chōfu, Tokyo
JAPAN

Printed in Japan